

# Tuning of the cosmic-ray test system of the BESIII drift chamber

WU Zhi(吴智)<sup>1,2;1)</sup> LIU Jian-Bei(刘建北)<sup>1</sup> QIN Zhong-Hua(秦中华)<sup>1</sup> WU Ling-Hui(伍灵慧)<sup>1</sup>  
 CHEN Chang(陈昌)<sup>1</sup> CHEN Yuan-Bo(陈元柏)<sup>1</sup> CHEN Ma-Li(陈玛丽)<sup>1</sup> CHEN Xi-Hui(陈锡辉)<sup>1</sup>  
 DONG Ming-Yi(董明义)<sup>1</sup> GUAN Bei-Ju(关北菊)<sup>1</sup> HUANG Jie(黄杰)<sup>1</sup> JIANG Xiao-Shan(江晓山)<sup>1</sup>  
 JIN Yan(金艳)<sup>1</sup> LI Fei(李飞)<sup>1</sup> LI Ren-Ying(李仁英)<sup>1</sup> LI Xiao-Nan(李小男)<sup>1</sup>  
 LEI Guang-Kun(雷广坤)<sup>1</sup> LIU Rong-Guang(刘荣光)<sup>1</sup> LUO Xiao-Lan(罗小兰)<sup>1</sup>  
 MA Xiao-Yan(马骁妍)<sup>1</sup> SHENG Hua-Yi(盛华义)<sup>1</sup> SUN Han-Sheng(孙汉生)<sup>1</sup> TANG Xiao(唐晓)<sup>1</sup>  
 WANG Lan(王岚)<sup>1</sup> WANG Liang(王靓)<sup>1</sup> XU Mei-Hang(徐美杭)<sup>1</sup> ZHANG Jian(张建)<sup>1</sup>  
 ZHANG Hong-Yu(章红宇)<sup>1</sup> ZHANG Yin-Hong(张银鸿)<sup>1</sup> ZHAO Yu-Bin(赵豫斌)<sup>1</sup>  
 ZHAO Ping-Ping(赵平平)<sup>1</sup> ZHU Ke-Jun(朱科军)<sup>1</sup> ZHU Qi-Ming(朱启明)<sup>1</sup> ZHUANG Bao-An(庄保安)<sup>1</sup>

<sup>1</sup> Institute of High Energy Physics, Chinese Academy of Sciences, Beijing 100049, China

<sup>2</sup> Graduate University of Chinese Academy of Sciences, Beijing 100049, China

**Abstract** The BESIII drift chamber and its subsystems need a cosmic-ray test after the chamber construction to check the chamber construction quality, testing the joint operation of the whole system and the performance of the chamber. The noise performance, drift time and charge measurements, and the scanning of channels were examined specifically. The preliminary results of the test indicate that the whole system works well.

**Key words** BESIII drift chamber, cosmic-ray test system, tuning

**PACS** 29.40.Gx

## 1 Introduction

The drift chamber [1] is the central tracking system of the BESIII experiment, operating in a 1 T magnetic field. In order to meet physical requirements, the drift chamber was designed as a small-cell, low-material cylindrical chamber filled with helium-based gases.

The radial extent of the drift chamber is from 59 to 810 mm, the length is 2308 mm, as shown in Fig. 1. Each endplate consists of an inner section, a stepped section and an outer section respectively. Both the inner and outer sections are machined from an integrated aluminum plate, respectively, and a multi-stepped conical structure is used. The stepped section is assembled from a set of 6 aluminum rings interconnected with nonmagnetic steel bands via radial screws. Both the inner and outer skins are made of carbon fiber.

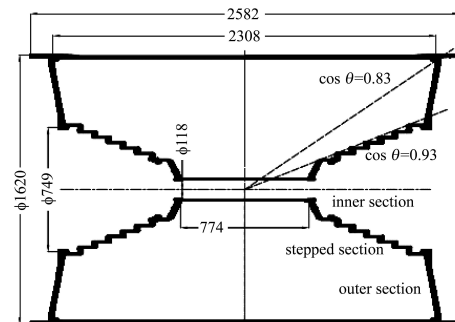


Fig. 1. Vertical cross-section of the BESIII drift chamber. The lengths are in units of mm.

There are 43 circular layers consisting of 6796 drift cells. 8 stereo sense wire layers are located in the inner section, the following 12 axial sense wire layers are located in the stepped section, and 16 stereo and 7 axial sense wire layers are arranged in the outer section. The drift cell adopts almost square shape. The space between sense and field layers is carefully

Received 15 August 2009, Revised 23 September 2009

1) E-mail: wuz@ihep.ac.cn

©2010 Chinese Physical Society and the Institute of High Energy Physics of the Chinese Academy of Sciences and the Institute of Modern Physics of the Chinese Academy of Sciences and IOP Publishing Ltd

adjusted by the simulation to keep uniform gas gain [2]. Since the track density is much higher at small radii, the choice of the half-cell size is 6 mm for the 8 inner layers to reduce the aging effect, and 8 mm for the following 35 layers. The sense wires are 25  $\mu\text{m}$  gold-plated tungsten while the field wires are 110  $\mu\text{m}$  gold-plated aluminum. Two sides of the wires are fixed at the holes in endplates by feedthroughs made up of a high voltage insulator and a crimp pin. The working gas is chosen to be  $\text{He}/\text{C}_3\text{H}_8(60/40)$ , which, together with the use of other low-mass materials, minimizes multiple scattering.

After the finished chamber construction, the drift chamber and its subsystems need a system test to check the joint operation of the whole system and the performance of the chamber. In this paper, we report the tuning of the BESIII drift chamber test

system with the cosmic-ray test. The installation of the front-end electronics is the key part of the preparation work. Noise reduction and channel scan were carried out during the tuning process.

## 2 The cosmic-ray test system

The cosmic-ray test of the chamber without magnetic field was carried out in a clean room, the temperature of which was kept at  $22\pm 1^\circ\text{C}$  to protect the wires. The system layout is shown in Fig. 2. The drift chamber was placed in the wiring machine for replacing bad wires if needed. To trigger the passing particles, four pairs of scintillation counters were placed above and under the chamber separately at a distance of 2.4 m. In order to scan all the channels, the counters can be moved accordingly.

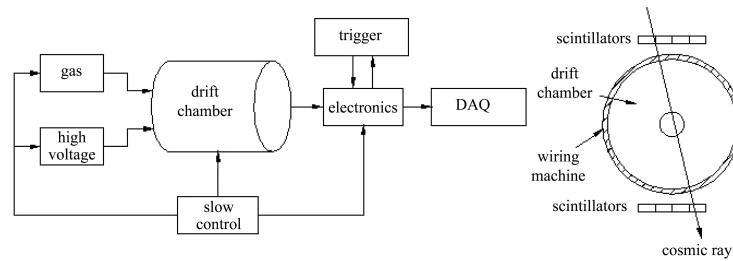


Fig. 2. The cosmic-ray test system layout of the BESIII drift chamber.

The high voltage system [3] consists mainly of the high voltage(HV) power supply, the HV distribution crate, the high voltage boards and cables for the connection. The high voltage is filtered at the distribution crate and fanned out to each HV board. There is also a filter circuit on each HV board before the HV is fanned out to 8 sense wires through a shielded wire.

The readout electronics [4] are composed of 853 preamplifiers, a 6U and sixteen 9U VME crates as shown in Fig. 3. A preamplifier board and a HV board mentioned above, called the front-end board, are designed in the same board and separated by a 1000pF capacitor and a 5 M $\Omega$  resistor, mounted on the two endplates with the odd layers on one side and the even layers on the other side. The 6U VME crate consists of the VME controller of the PowerPC750, the trigger and the clock production modules of CBT-I and CBT-II, the calibration and system control circuit of MCC, and the TDC module. The 9U VME crate consists of the readout control module of MROC, the fan-out module of MF-II, and the MQT modules. The MQT module is the key part of the

electronics system for time measurement and charge measurement.

The gas system consists of the gas supply bottle, mass flow meters, tank and proportional counters, etc. The gas ratios are controlled by mass flow meters, which first flow into a buffer tank from which it is supplied to the chamber at a rate of 6000 ml/min. There are 8 inlets and 8 outlets for the gas supply. In order to make sufficient heat exchange with the outer environments, 15 m copper pipes are chosen to connect the tank and the chamber. Plastic pipes are chosen for the output of the gas. Two cylindrical proportional counters are installed at the inlet and outlet of the chamber to monitor the gas mixture.

The air temperature and humidity inside the detector and at the front-end electronics are also monitored by sensors.

The hardware described above is controlled and monitored by the Slow Control System(SCS) [5]. An Ethernet connection is used for the communication between the HV crate and the top level software. The VME crates have a CANBUS interface for communication with the computer. A Siemens PLC is used

to switch on/off the mass flow meters by monitoring the gas pressure limit. To acquire data from the sensors, two types of DAQ boards and a USB/RS485 converter have been developed. The top level super-

visory and control software of the hardware systems is mainly developed by LabVIEW, MySQL and OPC Server. The SCS monitors and controls many parameters and can raise alarm if needed.

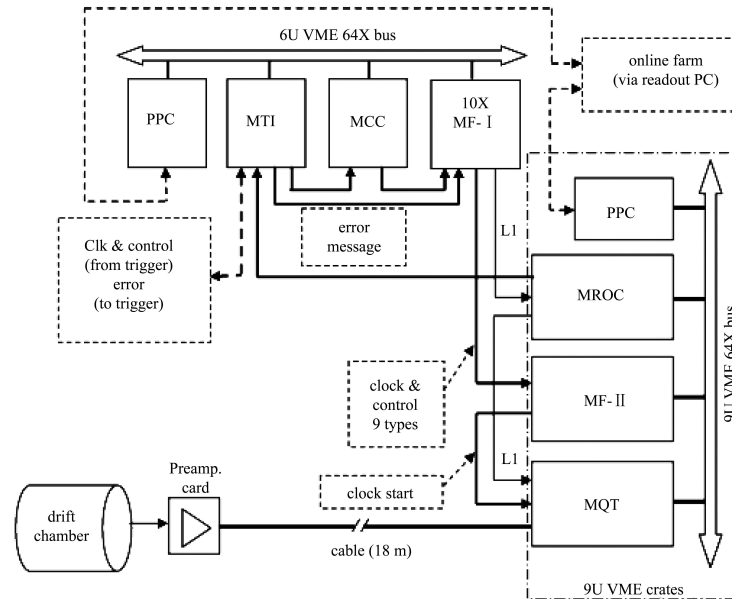


Fig. 3. The cosmic-ray layout of the BESIII drift chamber.

The data acquisition system works as follows: collecting event data from the electronics after the trigger; transferring data fragments from each VME readout crate to the online computer farm; assembling data fragments into event data, filtering the event data, and then recording the selected event into the disc. The running status is controlled and monitored by a program of the online PC to give real-time information to the operator.

### 3 Tuning of the cosmic-ray test system

The installation of the front-end boards is very important because they won't be disassembled after the test and the quality of assembly has a direct impact on the future operation. The system tuning was carried out after the system installation, including the noise reduction, adjusting electronics parameter, channel scan and so on.

#### 3.1 The installation of the front-end boards

For the installation of the front-end boards, the quality control procedures are as follows:

1) Before the installation, each front-end board must be tested at a voltage of 2300 V lasting more than 10 hours. The required dark current is less than

10 nA for each board.

2) The connection between the sense wires and the boards must be very careful to prevent potential damage to the feedthroughs or the wires. Make sure that the boards installed are in the correct position and have a good contact with the feedthroughs.

3) After step two, the HV training process was done for each board installed. The test was done with operating gas at high voltage of 2200 and 2300 V for the inner and outer chamber respectively. It lasts at least two hours and the required dark current is less than 10 nA for one board.

This work lasts 40 days, and the following problems are found and fixed:

1) Before the installation, the failed boards for high dark current would be treated and trained for another ten hours and would be rejected if failed again. These bad ones were mainly caused by damaged wires or connectors or dirt on the surface of the boards.

2) During the installation process, a series of wires couldn't be supplied with the nominal voltages. By the rigorous analysis and check, a broken field wire located at the outmost field layer of the inner chamber was found. These wires were normal when the broken wire was extracted.

3) During the training process, some wires in the first step had large dark currents. The current was up to several  $\mu\text{A}$  for the single wire. The reason was

that the sealants named Loctite 222 used in the chamber sealing have good flow and infiltration qualities. The glue wouldn't fix under aerobic conditions and had a weak conductivity. The sealant remnant was erased and pure nitrogen gas used to blow the stepped surface accelerated the remnants' fixture. Finally the dark current was less than 15 nA for the single wire.

4) In each aluminum ring of the stepped section, the dark current in the even sense layer is higher than that in the odd layer. The reason is that the even layer is very close to the steel band used to interconnect the different steps and there is a weak discharge between the two. The surface of the band facing the sense wire layer were treated with Kapton tape, then the dark current reduced dramatically.

### 3.2 Noise reduction

By quality control during the installation process, the front-end board had a low background noise and its output was less than 8 mV. However, when the chamber worked at the nominal voltages, the noise of some channels observed with an oscilloscope was very large and even saturated, having actuated signals on the adjacent channels. The reason is that during the stringing of the chamber, in order to mark the first channel of each board for convenience of the installation of the front-end boards, the insulator of the feedthrough was coated with a heat-shrinkable tube. The distance between the grounding screw of the board and the marking insulator is about 2 mm. There was discharge between the crimp pin of the feedthrough and the grounding screw through the tube. After getting rid of these marks, the system noise dropped to the acceptable level.

### 3.3 Electronics parameter adjustment

Both of charge and time measurements are required for each signal wire. A search window and a trigger latency are the important parameters for the time measurement. The search window should be opened with the width slightly larger than the maximum drift time, then set at the value of 700 ns. The trigger latency is adjusted by scanning drift time spectra to cover the maximum drift time. The trigger latency for the charge measurement is similar with that for time measurement, due to the circuit design. The charge measurement adopts a scheme based on FADC and extracts the charge value through a numerical integration. Since the shaped width of a signal has been determined to be about 1.3  $\mu$ s, 1.5  $\mu$ s is a reasonable choice. The main basis of threshold selection for the charge measurement is suppression of

the noise without signal loss. Fig. 4 give the drift time and charge spectra after the adjustment described above. The time spectra cover the maximum drift time within the time window. The rapid rise of the leading edge indicates a good time resolution. The width between the leading and falling edge of the time spectra is about 300 ns, which corresponds to the half-cell size. The well-known Landau tail of the charge spectra is due to the large fluctuation in the

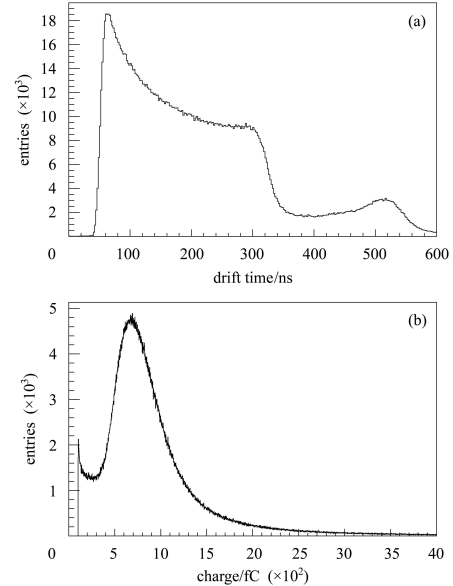


Fig. 4. Drift time (a) and charge spectrum (b).

ionization energy loss when charged particles pass through a thin gas volume. The enhancement at low charge values mainly consist of the noise hits. These results indicate that the whole system can work properly.

### 3.4 The grounding of boundary field layers

An additional field wire layer is arranged between the axial super-layer and the stereo super-layer to reduce the change of cell shape along the wires and then keep uniformity of the electric field. In the design positive compensating voltages of 100-200 V were applied to the boundaries to reduce the left-right asymmetry of the  $x-t$  relations [6]. During the debugging phase we found that the noise in the boundary layers is larger than other layers. The reason is that the voltages supplying the boundaries are connected to the field wires directly without a second filter, which is easy to induce noise after filtering at the distribution crate. So we abandoned the previous design and treated these layers with the proper grounding, the level of the noise dropped to the non-boundary layer's level. The left-right asymmetry of the  $x-t$  relations can be dealt with by off-line calibration.

### 3.5 The scanning of channels

The first data taking was done for the calibration to check whether the electronic chain (front-end electronics, cables, MQT) worked correctly. Data taking with cosmic-rays was operated subsequently. Some dead and hot channels have been found by checking the TDC and ADC spectra of each channel. The reason causing the dead channels are mainly as follows:

1) bad connection between the feedthrough and signal cable or HV cable.

2) damage of preamplifiers.

3) damage of the 3k filter resistance on the front-end boards, which can lead to 8 dead channels at a time. For the safe operation the 3k resistances of the front-end boards in the inner and stepped section were replaced by resistances withstanding higher voltages.

A sense wire in layer 42 is disconnected due to the large dark current. Other dead channels are all fixed. The hot channels caused by the abnormality of the preamplifier was replaced. Temperature sensors embedded into the detector also cause hot channels. The hot channels were fixed by grounding and shielding the cable of the sensors and keeping the cable at some distance from the front-end boards.

The abnormal spectra of channels are usually due to bad connections or malfunction of the electronics. These channels were solved by replacing the preamplifiers.

### 3.6 Performance of the electronics

The threshold for time measurement is the important parameter to be optimized, and is the main content of the chamber performance test. The cosmic-ray incident at the top of the terrestrial atmosphere includes muons, stable charged particles and nuclei with lifetimes of order  $10^6$  years or longer. A large amount of cosmic-ray sample with broad momentum range is acquired by the chamber during the data taking. In the cosmic-ray sample, muons are the most numerous charged particles. A good spatial resolution of  $128 \mu\text{m}$ , averaged over all the cells, is extracted from a dual-gaussian fitting to the residual distribution [7] as

shown in Fig. 5. Fig. 6 shows the efficiency as a function of the drift distance. The single-cell efficiency is over 97% in the middle region between the sense wire and the field wire while drops near the sense wire and the cell edge due to a very non-isochronic charge collection, which leads to the smaller signal. These results indicate that the drift chamber system functions according to expectations.

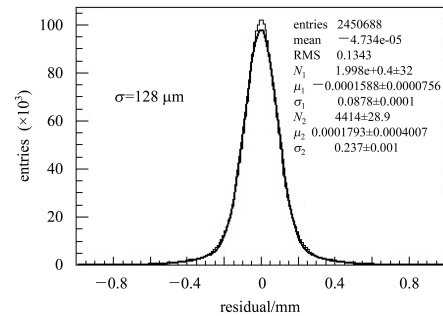


Fig. 5. Residual distribution.

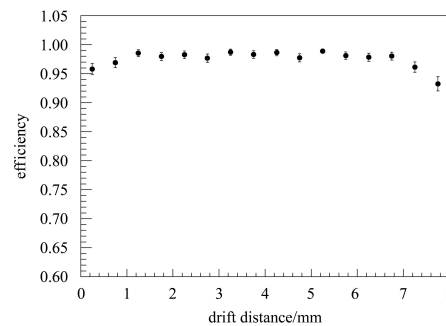


Fig. 6. Cell efficiency as a function of the drift distance.

## 4 Conclusions

The tuning of the BESIII drift chamber by the cosmic-ray test is successful. The installation of the front-end boards is a key part in order to guarantee the performance of the chamber. After the treatment of grounding, shielding and other effective methods, the noise reduced to a low level. By the channel scan the problematic channels were found and solved (except one dead channel unsolved, see section 3.5). From this system test it indicates that the whole system functions normally.

## References

- 1 BESIII Collaboration. BESIII Preliminary Design Report, 2004
- 2 WU Ling-Hui et al. HEP & NP, 2005, **29**(5): 476–480 (in Chinese)
- 3 XU Mei-Hang et al. Nuclear Electronics & Detection Technology, 2006, **26**: 199 (in Chinese)
- 4 QIN Zhong-Hua et al. Nucl. Instrum. Methods. A, 2007, **571**: 612
- 5 CHEN Xi-Hui et al. Chinese Physics C, 2007, **32**: 649
- 6 WU Ling-Hui et al. HEP & NP, 2006, **30**(7): 665–669 (in Chinese)
- 7 LIU Jian-Bei et al. Nucl. Instrum. Methods. A, 2006 **557**: 436